

**Title: Non-Destructive Evaluation of the mechanical strength of a TA6V4-Composite bonding using LASAT.**

**Author: Simon BARDY – CEA, DAM, DIF F-91297 Arpajon, France**

**Co-Authors:**

**Mathieu DUCOUSSO – Safran Tech, Rue des jeunes Bois, 78114 Magny les Hameaux France**

**Tomas BERGARA – Rescoll, 8 Allée Geoffroy Saint Hilaire, 33600 Pessac**

**Laurent BERTHE – Laboratoire Procédés et Ingénieries en Mécanique et Matériaux, CNRS, Arts et Métiers Paris Tech, 151 Bd de l'Hôpital, 75013 Paris, France**

**Laurent VIDEAU – CEA, DAM, DIF F-91297 Arpajon, France**

**Frédéric JENSON – Safran Tech, Rue des jeunes Bois, 78114 Magny les Hameaux France**

**Nicolas CUVILLIER – Safran Tech, Rue des jeunes Bois, 78114 Magny les Hameaux France**

**Speaker: Simon BARDY – CEA,DAM,DIF F-91297 Arpajon, France**

**Summary:**

In the current context of aircrafts' weight reduction and considering the trend for lowering production and maintenance-related costs, aeronautics industry promote the use of adhesive bonds to replace mechanical fasteners. However, the main limitation of structural bonding into aircraft industry concern the ability to certify in a non-invasive way the good quality of a structural bonding, i.e. to certify that the bonding can resist up to a predefined strength value. Conventional Non-Destructive Testing (NDT) techniques allow debonding detection but are inefficient to evaluate bond mechanical strength, i.e. weak bonds detection. The LASer Adhesion Test (LASAT) [1] is seen as a promising alternative to classical NDT techniques in order to reveal those weak bonds in a reproducible and automated way. It aims to apply calibrated mechanical stresses to a given bonded assembly using laser-induced shock waves. This calibrated configuration should lead to debonding of the joint/substrate interface in case of a weak bond and should not damage a healthy bond. Previous studies demonstrated the ability of the LASAT technology to characterize the quality of composite/composite bonded assemblies on typical operational thicknesses [2]. In this work, LASAT is applied to two levels of adhesive bond mechanical strength for a TA6V4/3D woven carbon/epoxy composite assembly. We will show the potential of this technology for such configuration.

## 1- Introduction

Amongst NDT Techniques, different methods are investigating the possibility of quantifying mechanical strength of structural bonding. However, a lot of different defects can diminish the quality of the bond and some of them are very difficult to detect. There is therefore a need for developing a new test method, based on acoustic approach to solicit and detect weak bonds. In this work, the ability of the LASer Adhesion Test method [1] to reveal weak bonds in Titanium – 3D Composite bonds is investigated.

## 2- LASAT principle

The LASAT technique is based on the following principle: a high energy ( $E$ ) pulsed laser beam is focused on some mm<sup>2</sup> of focal spot ( $S$ ) on a given target front face for time duration ( $\tau$ ) of several ns. The laser pulse can therefore be characterized by its intensity (Eq. 1).

$$I \left( \frac{GW}{cm^2} \right) = \frac{E (J)}{\tau (ns) * S (cm^2)} \quad \text{Eq. 1}$$

Due to collisional absorption and inverse Bremsstrahlung phenomena [3], the matter is quickly heated up to vapor and plasma state. In application of the Newton's third law, the ejection of matter from the front face in direction of the laser beam leads to the creation of a reaction force in the opposite direction, i.e. towards the sample.

Using a confining dielectric layer, such as water, has been identified for a long time as an optimization technique to generate shocks with smaller laser intensities [4] (Fig. 1). The use of this type of geometry prevents plasma expansion and hence maximizes both shock amplitude and duration. Nevertheless, it must be kept in mind that water breakdown plasma occurs at intensities around 10 GW/cm<sup>2</sup>, depending on laser pulse duration and wavelength [5]. This phenomenon limits to some GPa the maximal ablation pressure which can be applied to a target.

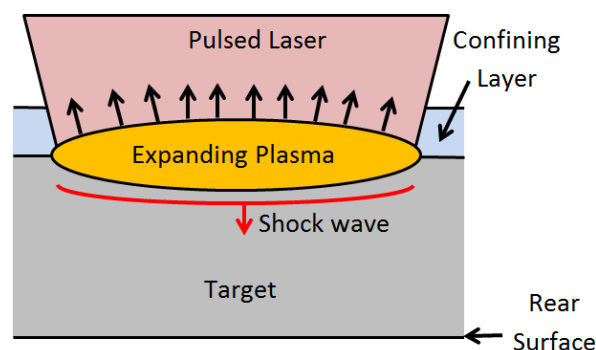


*Fig. 1: Schematic view of the generation of a shockwave induced by laser in confined geometry*

The amplitude (some GPa) and duration (some ns) of the resulting loading, named ablation pressure ( $P_{abl}$ ), imply strong temporal and spatial discontinuities, typical of a shock wave. The maximum ablation pressure can be estimated thanks to well-known analytical laws [6] or even using validated laser-matter interaction codes [7].

The shock wave generated in the front face propagates then through the thickness of the sample. Following acoustic impedance transmission-reflection laws, tensile stresses zones can be generated thanks to release waves recombination. If the applied tensile stress is higher than the dynamic mechanical resistance of the bonding, then cohesive or adhesive fracture of the bonding is observed. Use of conventional NDT techniques as post-shock evaluation is however necessary to determine which laser shots lead to disbonding. The LASAT technique coupled to a disbonding diagnostic can therefore be seen as a proof test since the use of a calibrated laser pulse should discriminate weak bonds from healthy bonds. The main challenge for industrial applications stays the non-destructive side of the LASAT which must be proven. In this work we bring some serious results assessing for the NDT capacity of the technique.

### 3- Experiments

- Materials

The samples investigated here are TA6V-3D woven composite bonded together with a typical aeronautic epoxy glue. The respective thicknesses of the titanium, the glue and the composites are 0.4 mm, 0.150 mm and 3.8 mm for the considered samples. Lateral dimensions of the bonding are 240x40 mm<sup>2</sup>.

Two different mechanical grades of bonding quality were achieved by varying glue reticulation during curing step. Mechanical properties of the obtained bond quality were investigated using typical static mechanical testing methods. Results are given in *Table 1*.

*Table 1: Mechanical strengths of samples.*

	Good bond	Weak bond
Shear Mechanical Strength	35 MPa	15 MPa
Longitudinal Mechanical Strength	39 MPa	10 MPa

As expected, the good bonding exhibits resistance to failure larger than weak bond. Weak-to-good properties were expected to be about 50%. We see here that depending on the mechanical solicitation, results differ significantly.

- Laser Facility

LASAT experiments were performed on the Hephaistos facility at the ENSAM-Paris PIMM (Procédés et Ingénierie en Mécanique et Matériaux) laboratory. This installation enables 7-ns FWHM Gaussian pulses in the visible wavelength spectrum (532 nm). This Thales Gaia HP laser is capable of generating up to 14 J which can be deposited on target in a single pulse.

In our experiments, the Hephaistos laser beam was focused on the front face of the material, either TA6V4 or 3D-Composite face (*Fig. 2*). Water confined regime was employed to maximize the applied pressure. Back face velocity monitoring using PDV system [8] was achieved to follow the main back and forth of shock waves travels within the sample thickness.

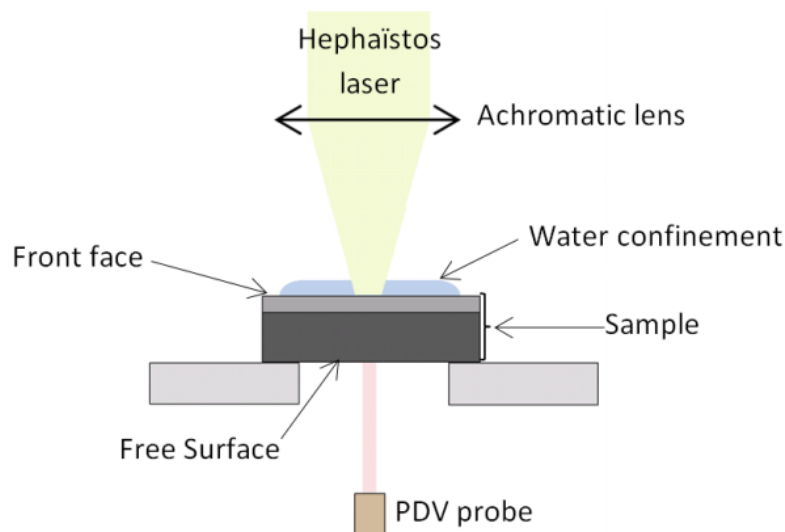


*Fig. 2: Laser Adhesion Test configuration*

- Description of the applied procedure

Disbonding thresholds were investigated on both mechanical strengths. Using 2 samples for each mechanical grade enabled also to investigate both TA6V and Composite front face configuration, *i.e.* to see what could be the influence of the impacted face on the disbonding threshold. Lateral dimensions of the samples enable about 10 laser shots per sample (*Fig. 3*). This repartition enables to have about 20mm between each laser spot, guarantying no influence of one shot on the others. The focal spot diameter was chosen to be 6mm-large in order to maximize the induced disbonding size, and hence their detectability. This geometry permits also to reach intensities just beyond the water breakdown threshold, see. *Eq. 1*, and thus maximize the ablation pressures used. In addition, focal spot diameter to thickness ratio stays relatively high, ensuring 1D shock propagation. In each bonding quality – front face configuration, gradual intensities were applied from 0.5 GW/cm<sup>2</sup> to 6 GW/cm<sup>2</sup>.



*Fig. 3: Front face of TA6V-Composite sample after laser ablation*

After LASAT experiments, ultrasonic inspection in water immersion with transmission configuration was employed to detect laser-induced disbonding. Emitting traducer was working at 15MHz and reception was achieved with help of 10 MHz sensor.

**4- Results**

- Disbonding thresholds

Laser shots are referenced in Fig. 4 for each configuration with their corresponding intensity and ultrasonic (US) evaluation of the bond state. Disbonding thresholds are identified and given in Table 2. Uncertainty on threshold is considered as only impacted by the uncertainty on laser energy, which is about 10%.

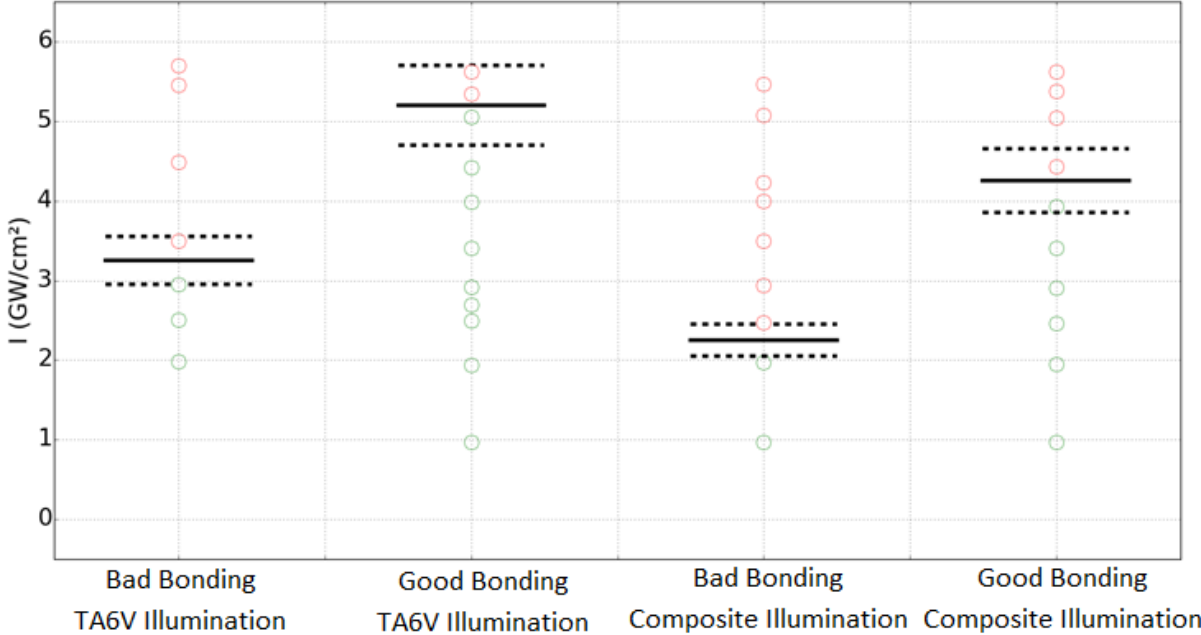


Fig. 4: Summary of laser shots for each configuration with US debonding diagnostic (green circles – no debonding detected, red circles - debonding detected) and debonding thresholds in black lines (uncertainty on threshold is indicated with dotted lines)

Table 2: Disbonding thresholds identified by US inspection after LASAT

	TA6V illumination	Composite illumination
Good Bond	<b>5.2 GW/cm<sup>2</sup></b> (+/- 0.5 GW/cm <sup>2</sup> )	<b>4.25 GW/cm<sup>2</sup></b> (+/- 0.4 GW/cm <sup>2</sup> )
Weak Bond	<b>3.25 GW/cm<sup>2</sup></b> (+/- 0.3 GW/cm <sup>2</sup> )	<b>2.25 GW/cm<sup>2</sup></b> (+/- 0.2 GW/cm <sup>2</sup> )

First, we notice that whatever the illumination side is, disbonding thresholds are clearly different for good bonds and for weak bonds. This shows the potential of LASAT technique to identify weak bonds by applying a calibrated laser pulse, above the weak bond threshold and beyond the nominal bond threshold. As an example, illuminating such a sample with a 4GW/cm<sup>2</sup>-pulse on the TA6V must release a good bond intact and induce a disbonding in a weak bond. Post-shock US scanning would reveal the eventual presence of disbonding and hence determine if the sample is a good bond or not.

We notice a slight difference whether the shock is generated on the TA6V or on the composite side. We believe this difference is implied by different patterns of waves' propagation within samples.

- Time-Position Diagrams

Some simulations were realized using a 1D-hydrodynamic code with simple material models. These simulations enabled the Time-Position (X-t) diagram corresponding to 3GW/cm<sup>2</sup> experiments. An equal laser loading (ablation pressure) is applied at t=X=0 for both configurations: TA6V illumination and Composite illumination. Tensile stresses in the joint appear at different time, regarding the type of configuration which is used, in relation with impedance mismatch in the three layers ( $Z_{\text{Epoxy}} = 3 \cdot 10^6 \text{ Pa} \cdot \text{s}^{-1}$ ,  $Z_{\text{Composite}} = 5 \cdot 10^6 \text{ Pa} \cdot \text{s}^{-1}$  and  $Z_{\text{TA6V}} = 15 \cdot 10^6 \text{ Pa} \cdot \text{s}^{-1}$ ).

In the case of composite irradiation (*Fig. 5*), the incident shock waves traveling in the composite interacts with the Composite/Epoxy interface (X=-3.8mm). Due to relatively closed acoustic impedances on each side of this interface, the amplitude of the reflected release wave ( $Z_{\text{Composite}} > Z_{\text{Epoxy}}$ ) is rather small and most of the incident energy is transmitted as shock wave in the epoxy layer. The resulting transmitted wave in the Epoxy layer is a shock wave which interacts then with the Epoxy/TA6V interface (X=-3.95mm). The reflected wave is a shock wave ( $Z_{\text{Epoxy}} < Z_{\text{TA6V}}$ ) going backward in the Epoxy layer and then in the composite. The transmitted wave at this interface is a shock wave propagating in the TA6V, which will then reflect itself as a release wave at the free surface on the back face of the material (X=-4.35mm – t=1100 ns). This release wave is partially reflected as shock wave at the TA6V/Epoxy interface as it goes backward and a corresponding transmitted release wave goes back in the epoxy layer and then in the composite. We can observe quick back and forth of shock waves which are trapped within the TA6V layer, due to high impedance mismatch between TA6V and Epoxy.

We can see that this propagation pattern generates successive release waves in the Epoxy layer between 1100 ns and 2000 ns which progressively induce tensile stresses in the bond by recombination with incident release waves. If the initial loading, *i.e.* laser ablation pressure, is sufficiently high, the resulting tensile stresses can exceed the bond and/or the Composite/Epoxy interface mechanical strength and hence generates a disbonding. We see here that maximal tensile stresses in the bond are reached after shock waves through the sample thickness (t=1500ns).

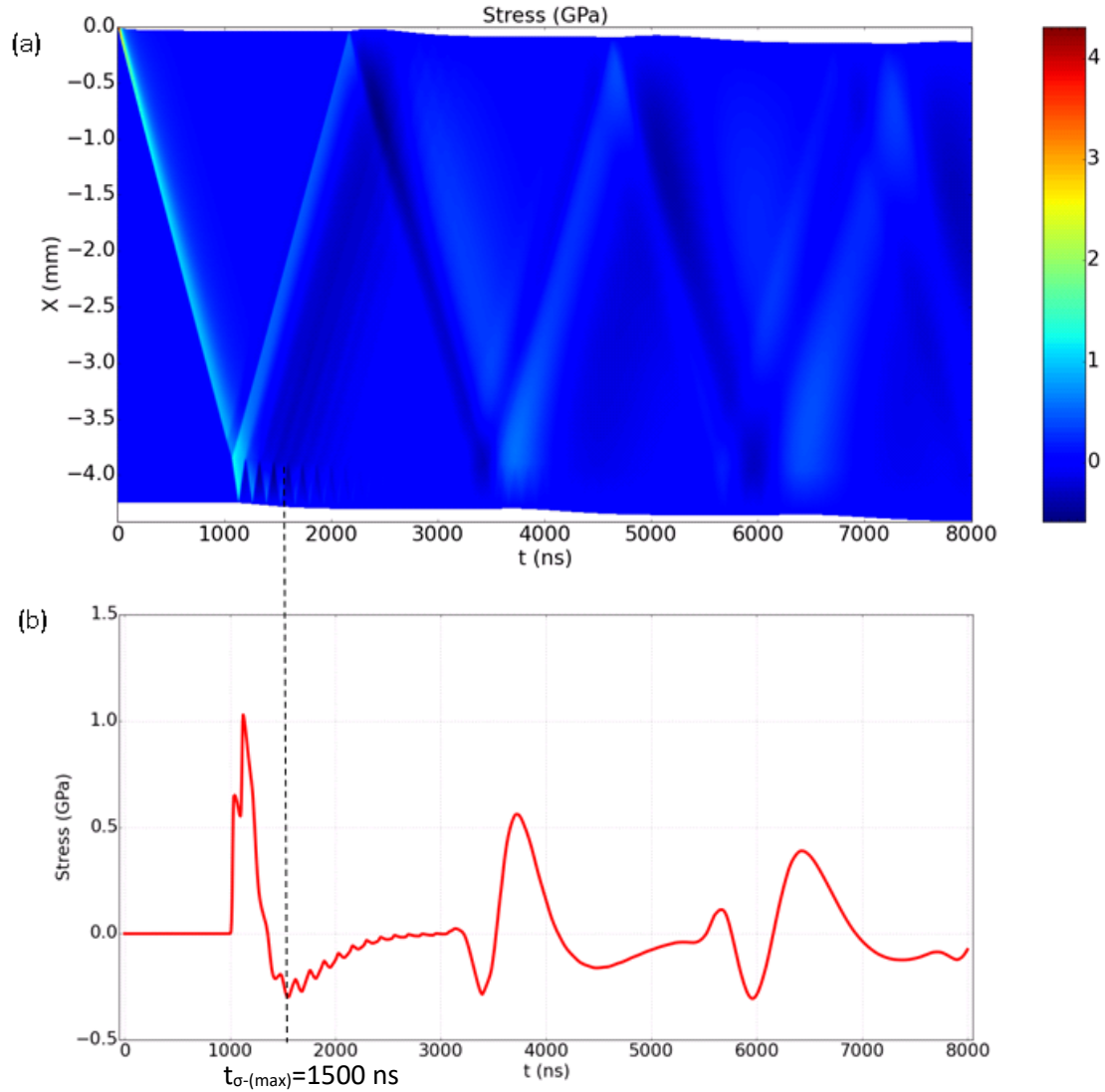


*Fig. 5: (a) Time-Position (X-t) diagram of stress and (b) Stress evolution at the Epoxy/Composite interface in the Composite illumination case*

In the case of TA6V irradiation (Fig. 6), the incident shock wave is generated in the TA6V and then partially transmitted as shock wave at the TA6V/Epoxy interface ( $X=-0.4$ mm). The reflected wave at this interface is a release wave ( $Z_{TA6V} > Z_{Epoxy}$ ) which goes back to the front face and reflects again as a shock wave in the TA6V layer. We see here that the shock waves pattern in the TA6V layer is very comparable to the one exposed in the Composite illumination configuration, except that in this case it generates successive shock waves in the rest of the sample. These shock waves travel in the epoxy layer and are transmitted as shock wave in the composite. Reflection of these shock waves at the Epoxy/Composite interface ( $X=-0.55$ mm) are neglected here, due to their small amplitude. The first incident shock wave in the composite reaches the composite free surface of the sample ( $X=-4.35$ mm –  $t=1100$ ns), where it is completely reflected as release wave. Recombination of this reflected release wave with incident ones lead to the creation of a tensile stress zone. This tensile zone goes then backwards and reaches the epoxy layer. As described previously, if the maximal tensile stresses exceed the bond and/or the Composite/Epoxy mechanical strength, disbond occurs.

However, it has to be noted that in that case, shock waves propagate twice through the composite before generating a maximum of tensile stresses at the interface ( $t=2500$  ns).

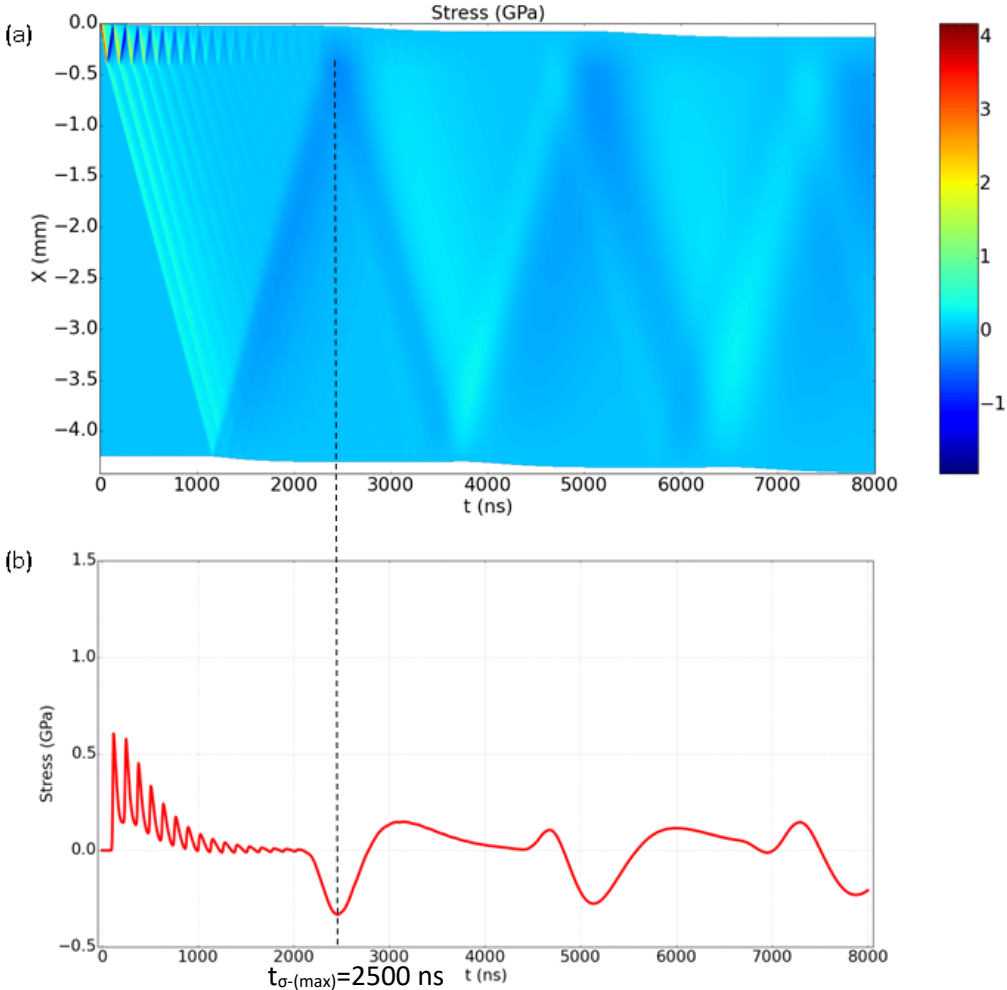
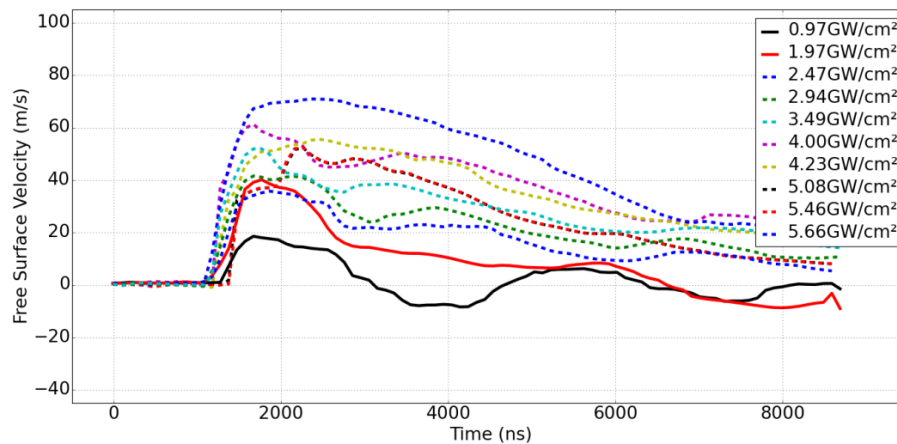


Fig. 6: (a) Time-Position (X-t) diagram of stress and (b) Stress evolution at the Epoxy/Composite interface in the TA6V illumination case

The shock wave propagation patterns shown here suggest the composite illumination side as an optimal configuration for the LASAT. Shock waves propagate on a shorter acoustic path in that configuration and hence are less subjected to attenuation through the composite. We believe that this accounts for the dependence of debonding thresholds to the illumination side. However, 2D or 3D simulations with a developed composite model, taking anisotropy into account, are wished. This should enable quantitative simulation of shockwave attenuation and thus give more precise stress evaluation within the stacking. Quantitative evaluation of bond mechanical strength could be obtained with the set of experimental data exposed here.

- Free Surface Velocity measurement

Free Surface Velocities (FSV) on the back face of sample showed also some interesting results. In the configurations concerned by laser illumination on composite side, a strong correlation between FSVs and ultrasonic diagnostic can be identified.



*Fig. 7: Evolution of the Free Surface Velocity with time for composite illumination shots on weak bond – Temporal resolution = 50 ns – Signals in dotted lines correspond to identified disbonding configurations*

In fact, FSVs recorded during experiments which lead to bond failure exhibits a spallation-type curve [9][10]. As an example, on *Fig. 7*, laser shot achieved at 0.97GW/cm<sup>2</sup> (black curve) shows clear back and forth of shock waves in the whole stacking. FSV is oscillating around 0 m/s. Negative FSV might be induced by 2-dimensionnal effects. The corresponding period of this type of event is about 3 μs, which is coherent with the longitudinal shock velocity of constitutive materials. Contrariwise, disbonding must imply a creation of a free surface at the TA6V/Epoxy interface, which means that this layer is not unloaded by release waves like the rest of the sample and therefore its FSV profile exhibits a quasi-constant velocity just after the main peak. Back and forth of shock waves in the TA6V layer must generate FSV oscillations after disbonding (*Fig. 5. (a)*). However, the temporal resolution of the PDV analysis used here (50 ns) must prevent these oscillations detection. It seems also that FSV curves might be impacted by 2-dimensionnal effects as negative values are visible in some cases. These edge effects are hardly understandable without appropriate simulation.

- Non-Destructive Testing

Finally, post-shock micrographs achieved on samples that had been submitted to the highest intensities did not reveal any failure in both composite or TA6V.

Separate characterization of both TA6V and 3D-Composite under laser shock in the same conditions (thicknesses, laser intensity) had already led to the same observation.

These observations show that in this case, laser-induced shocks seem to not have affected the material. The LASAT configuration used here seems to not have induced damage in substrates. Regarding the nature of the substrates and the respective thicknesses of materials, it seems that the LASAT configurations used in this study are non-destructive. Some deeper

investigations must be lead to assess the LASAT as non-destructive. Mechanical testing after laser shocks is planned to confirm the non-degradation of the substrates and the joint below their respective damaging threshold.

## **5- Conclusion**

- The LASAT configuration used here enables to discriminate a weak bond from a good bond with help of a disbonding diagnostic. In addition, the good bond disbonding threshold has been clearly identified. It means that a weak bond just beyond the tolerance (+/- 20% of the good strength) should also be discriminated using the same configuration. Some further experiments should be led with such a bond quality.
- In-situ Free Surface Velocimetry has given some encouraging results for the detection of disbonding in a given configuration. Deeper investigations should be lead with this technique to confirm its potential of disbonding detection coupled with laser-induced shock waves.
- Post-shock diagnostics confirm the potential of the LASAT to be non-destructive. However, it should be noticed that some modifications of the material due to the shock might be non-detectable, even with micrographs. Mechanical testing on samples subjected to laser shocks must be driven to demonstrate the non-destructive aspect of such technology.
- 1D simulation enabled to build Time-position diagrams necessary for understanding shock wave propagation patterns involved. Based on these tools, an interpretation of the disbonding threshold dependence to illumination side was proposed.
- 2D or 3D simulations must be realized to simulate more precisely attenuation phenomena and edge effects. Quantitative simulation could give more information on the evolution of stresses within substrates and, if needed, help to define a more optimized configuration to lower stresses in substrates, while still covering weak bonds detection application. In addition, mechanical resistance of bonds under shock loading could be determined by using such a code.

## References

1. L. Berthe et al., "State-of-the-art laser adhesion test (LASAT)," *Nondestructive Testing and Evaluation*, 26 (3-4), 303-317 (2011)
2. R. Ecault et al., "Development of a laser shock wave adhesion test for the detection of weak composite bonds," 5th International Symposium on NDT in Aerospace - Singapore (2013)
3. P. Mora, "Theoretical model of absorption of laser light by a plasma," *Phys. Fluids* 25, 1051 (1982).
4. N. C. Anderholm, "Laser-generated stress waves," *Appl. Phys. Lett.* 16,113 (1970)
5. A. Sollier et al., "Numerical modeling of the transmission of breakdown plasma generated in water during laser shock processing," *The Eur. Phys. J. AP* 16, 131-139 (2001)
6. R. Fabbro, "Physical study of laser-produced plasma in confined geometry", *Journal of Applied Physics* 68, 775 (1990)
7. S. Bardy et al. , "Numerical study of laser ablation on aluminum for shock-wave applications: development of a suitable model by comparison with recent experiments", *Opt. Eng.* 56, 011014 (2016)
8. O. T. Strand et al., Compact system for high-speed velocimetry using heterodyne techniques , *Review of Scientific Instruments* 77, 083108 (2006)
9. L. Tollier et al., "Study of the laser-driven spallation process by the velocity interferometer system for any reflector interferometry technique. I. Laser-shock characterization.", *Journal of Applied Physics* 83, 1224 (1998)
10. L. Tollier et al., "Study of the laser-driven spallation process by the VISAR interferometry technique. II. Experiment and simulation of the spallation process.", *Journal of Applied Physics* 83, 1224 (1998)